

# Accepted Manuscript

Chiral resolution, absolute configuration determination, and stereo-activity relationship study of IDO1 inhibitor NLG919

Wen-Qiang Liu, Fang-Fang Lai, Jie Zhang, Li Sheng, Yan Li, Li Li, Xiao-Guang Chen



PII: S0040-4020(18)30513-1

DOI: [10.1016/j.tet.2018.05.005](https://doi.org/10.1016/j.tet.2018.05.005)

Reference: TET 29512

To appear in: *Tetrahedron*

Received Date: 17 March 2018

Revised Date: 26 April 2018

Accepted Date: 2 May 2018

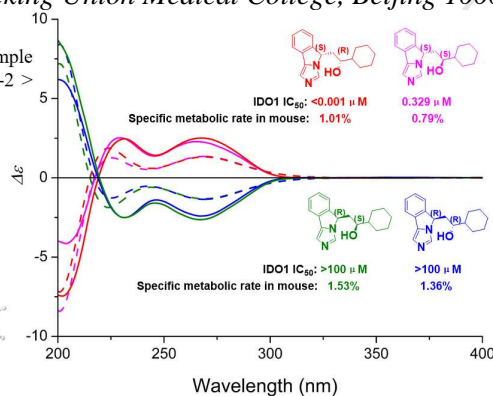
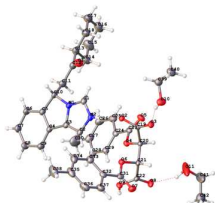
Please cite this article as: Liu W-Q, Lai F-F, Zhang J, Sheng L, Li Y, Li L, Chen X-G, Chiral resolution, absolute configuration determination, and stereo-activity relationship study of IDO1 inhibitor NLG919, *Tetrahedron* (2018), doi: 10.1016/j.tet.2018.05.005.

This is a PDF file of an unedited manuscript that has been accepted for publication. As a service to our customers we are providing this early version of the manuscript. The manuscript will undergo copyediting, typesetting, and review of the resulting proof before it is published in its final form. Please note that during the production process errors may be discovered which could affect the content, and all legal disclaimers that apply to the journal pertain.

## Graphical Abstract

**Chiral resolution, absolute configuration determination, and stereo-activity relationship study of IDO1 Inhibitor NLG919**

Leave this area blank for abstract info.

Wen-Qiang Liu<sup>#</sup>, Fang-Fang Lai<sup>#</sup>, Jie Zhang, Li Sheng, Yan Li, Li Li<sup>\*</sup>, Xiao-Guang Chen<sup>\*</sup>*State Key Laboratory of Bioactive Substance and Function of Natural Medicines, Institute of Materia Medica, Chinese Academy of Medical Sciences & Peking Union Medical College, Beijing 100050, China*Highly effective and simple chiral resolution of *rac*-2 > 99% ee, 70% yield



# Chiral resolution, absolute configuration determination, and stereo-activity relationship study of IDO1 inhibitor NLG919

Wen-Qiang Liu<sup>#</sup>, Fang-Fang Lai<sup>#</sup>, Jie Zhang, Li Sheng, Yan Li, Li Li<sup>\*</sup>, Xiao-Guang Chen<sup>\*</sup>

State Key Laboratory of Bioactive Substance and Function of Natural Medicines, Institute of Materia Medica, Chinese Academy of Medical Sciences & Peking Union Medical College, Beijing 100050, China

## ARTICLE INFO

### Article history:

Received  
Received in revised form  
Accepted  
Available online

### Keywords:

Indoleamine 2,3-dioxygenase 1 (IDO1) inhibitor  
Single crystal X-ray diffraction  
Optical resolution  
Absolute configuration  
Electronic circular dichroism

## ABSTRACT

NLG919 (**1**) with two chiral carbon atoms on its chemical structure is a potent indoleamine 2,3-dioxygenase 1 (IDO1) inhibitor. We developed an effective way to prepare all stereoisomers of **1**, the key step being the chiral resolution of racemic intermediate **2**. The optimal resolution solvent system was identified as dichloromethane and n-pentane or petroleum ether. Using (–)-di-p-toluoyl-D-tartaric acid as resolution reagent, optical pure (*R*)-**2** (e.e. > 99%, yield = 70%) was obtained. The mechanism of chiral resolution was clarified through single-crystal X-ray diffraction of the diastereomeric salt. The absolute configurations of four stereoisomers of **1** were established through electronic circular dichroism spectra, quantum chemical calculation and transition metal method. Their IDO1 inhibitory activity was assessed by pharmacological experiments in vitro and in mouse, demonstrating that *S* configuration of C5 played an important role on the inhibition of IDO1, while the stereochemistry on C2' exerted little effect on the IDO1 inhibitory activity in mouse.

2018 Elsevier Ltd. All rights reserved.

## 1. Introduction

Immune checkpoint therapies have become a research hotspot in cancer treatment<sup>1</sup>. Several immune checkpoint inhibitors have been approved by FDA and applied clinically<sup>2</sup>. Indoleamine 2,3-dioxygenase 1 (IDO1) is an intracellular heme-containing enzyme, which initiates the first and rate-limiting step of the L-tryptophan (L-Trp) degradation along the kynurenine (Kyn) pathway<sup>3</sup>. The depletion of L-Trp in tumor microenvironment would lead to an immunosuppressive effect, causing the immune escape of tumors<sup>4</sup>. Some IDO1 inhibitors have been reported, such as epacadostat, indoximod, and NLG919 (**1**, Fig. 1)<sup>5</sup>.

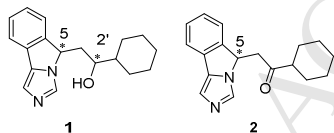


**Fig. 1.** Chemical structures of **1** and **2**.

It is reported that stereochemistry might affect the IDO1 inhibitory activity of NLG919<sup>6</sup>. Meanwhile, the preparation of stereoisomers of **1** need harsh reaction condition and give low yield<sup>7</sup>. Therefore, it is necessary to develop an effective way to prepare optical pure stereoisomers of **1** for pharmacology and pharmacokinetics study.

The classical enantiomer separation through the diastereomeric salt formation is a useful approach for large scale preparation of chiral molecules<sup>8</sup>. The synthetic intermediate (**2**, Fig. 1) contains an alkaline imidazole fragment and a carbonyl group, which could interact with resolution agents or solvents. Thus, it was possible to realize optical resolution of *rac*-**2** through the formation of diastereomeric salts with chiral organic acids.

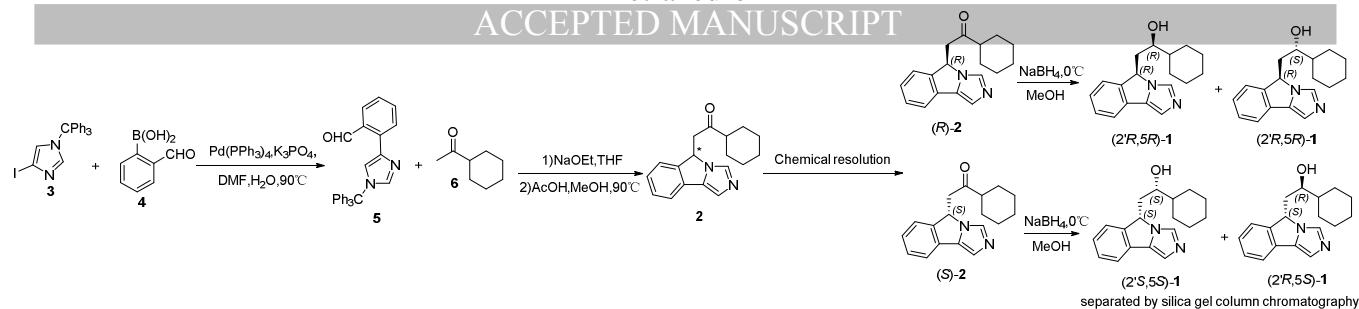
By using optical pure **7** as resolution agent, we achieved highly effective resolution of *rac*-**2**. Four diastereoisomers of **1** were then prepared by the reduction of **2** and column chromatography. The absolute configurations of stereoisomers were assigned by electronic circular dichroism (ECD) spectra combined with quantum-chemical calculations, and transition metal method. The chiral resolution mechanism was elucidated by the analysis of the diastereomeric salt crystal of (*S*)-**2**:*L*-**7** (CCDC 1570864). The pharmacological evaluation of stereoisomers of **1** in vitro and in vivo was also carried out. Herein, the results of our study will be reported.

## 2. Result and discussion

### 2.1. Synthesis and chiral resolution of *rac*-**2**

The synthesis route of optical pure diastereomers of **1** is displayed in Scheme 1. Firstly, *rac*-**2** was prepared through Suzuki reaction, condensation and cyclization reactions.

<sup>#</sup> W.-Q. Liu and F.-F. Lai contributed equally to this work. <sup>\*</sup> Corresponding authors. Tel.: +86-10-63165247; e-mail: [annaleelin@imm.ac.cn](mailto:annaleelin@imm.ac.cn) (L. Li); e-mail: [chxg@imm.ac.cn](mailto:chxg@imm.ac.cn) (X.-G. Chen).



**Scheme 1.** Synthesis route of optical pure diastereomers of **1** through chiral resolution of *rac*-**2**.

Five commercially available and commonly used acidic resolving agents **3-7** (Fig. 2) were screened for the enantiomer resolution of *rac*-**2**. Firstly, *Rac*-**2** and resolving agents were mixed and dissolved in ethanol (EtOH) for crystallization (Table 1, entries 1-5). Only when using **D-7**, a small amount of needle-like precipitation appeared with low enantiomeric excess (entry 5, (*R*)-**2**, e.e. = 15.62%). However, when the mixture solvent based on EtOH was used, no precipitation appeared (entry 6). Other resolving agents could not form solid with *rac*-**2**, even after removing the solvent. It is thus deduced that the resolution agents with large aromatic group are suitable for the resolution of *rac*-**2**, and the methyl group of **7** might play an important role in the process of chiral recognition.

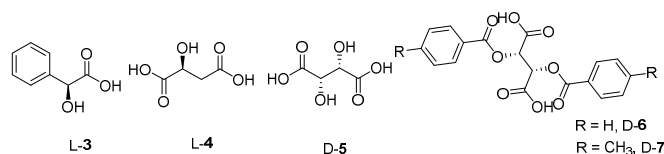


**Fig. 2.** Acidic resolving agents used in this study.

**Table 1.** Chiral resolution of *rac*-**2** with acidic resolving agents<sup>a</sup>

Entry	Resolving agent	Conditions <sup>b</sup>	e.e. (%) <sup>c</sup>
1	L-3 (2.0 equiv.)	EtOH (2.0 L/mol) <sup>c</sup>	- <sup>d</sup>
2	D-4 (2.0 equiv.)	EtOH (2.0 L/mol) <sup>c</sup>	- <sup>d</sup>
3	L-5 (2.0 equiv.)	EtOH (2.0 L/mol) <sup>c</sup>	- <sup>d</sup>
4	D-6 (2.0 equiv.)	EtOH (2.0 L/mol) <sup>c</sup>	- <sup>d</sup>
5	D-7 (2.0 equiv.)	EtOH (2.0 L/mol) <sup>c</sup>	15.62 (R)
6	D-7 (2.0 equiv.)	EtOH:H <sub>2</sub> O = 6:1 (4.2 L/mol) <sup>c</sup>	- <sup>d</sup>

<sup>a</sup> The amount of *rac*-**2** was 0.30 mmol. <sup>b</sup> The amount of solvent based on the amount of *rac*-**2** is shown within the parenthesis. <sup>c</sup> The process of heating to complete dissolution and cooling to room temperature for 2–24 h. <sup>d</sup> No crystallization. <sup>e</sup> e.e. was determined by chiral HPLC analysis.

## 2.2. Optimization of resolution conditions

By using other solvents such as methanol (MeOH), dimethyl sulfoxide (DMSO), ethylene glycol (EG), isopropanol (i-PrOH), ethyl acetate (EA), tetrahydrofuran (THF) and dichloromethane (DCM) (Table 2, entries 1-7), it was found that when polar solvents (MeOH, DMSO, EG, i-PrOH) was used, there was no precipitate (entries 1-4). However, when using low polar solvents (EA, THF, and DCM), there was still no resolution effect (entries 5-7). But, it was noticed that *rac*-**2** and **D-7** tended to form a solid without enantiomeric excess after removal of DCM under reduced pressure. Considering this unique phenomenon, further optimization of the resolution solvent was carried out based on the solvent of DCM.

**Table 2.** Optimization of the resolution conditions of *rac*-**2** with **D-7**<sup>a</sup>.

Entry	Resolving agent	Conditions <sup>b</sup>	e.e. (%) <sup>c</sup>
1	D-7 (2.0 equiv.)	MeOH (4.0 L/mol) <sup>c</sup>	- <sup>d</sup>
2	D-7 (2.0 equiv.)	DMSO (4.0 L/mol) <sup>c</sup>	- <sup>d</sup>
3	D-7 (2.0 equiv.)	EG (4.0 L/mol) <sup>c</sup>	- <sup>d</sup>
4	D-7 (2.0 equiv.)	i-PrOH (4.0 L/mol) <sup>c</sup>	- <sup>d</sup>
5	D-7 (2.0 equiv.)	EA (4.0 L/mol) <sup>c</sup>	- <sup>d</sup>
6	D-7 (2.0 equiv.)	THF (10.0 L/mol) <sup>c</sup>	- <sup>d</sup>
7	D-7 (2.0 equiv.)	DCM (10.0 L/mol) <sup>c</sup>	- <sup>d</sup>
8	D-7 (2.0 equiv.)	DCM:EtOH = 4:1 (8.3 L/mol) <sup>c</sup>	- <sup>d</sup>
9	D-7 (2.0 equiv.)	DCM:i-PrOH = 4:1 (8.3 L/mol) <sup>c</sup>	- <sup>d</sup>
10	D-7 (2.0 equiv.)	DCM:EA = 4:1 (8.3 L/mol) <sup>c</sup>	- <sup>d</sup>
11	D-7 (2.0 equiv.)	DCM:PE = 4:1 (8.3 L/mol) <sup>c</sup>	19.54 (R)
12	D-7 (2.0 equiv.)	DCM:PE = 8:1 (11.3 L/mol) <sup>c</sup>	55.78 (R)
13	D-7 (2.0 equiv.)	DCM:PE = 13:1 (14.3 L/mol) <sup>c</sup>	82.43 (R)
14	D-7 (2.0 equiv.)	DCM:PE = 17:1 (18 L/mol) <sup>c</sup>	71.57 (R)
15	D-7 (1.5 equiv.)	DCM:PE = 8:1 (11.3 L/mol) <sup>c</sup>	64.93 (R)
16	D-7 (1.5 equiv.)	DCM:PE = 13:1 (14.3 L/mol) <sup>c</sup>	87.21 (R)
17	D-7 (1.5 equiv.)	Wash once	96.32 (R)
18	D-7 (1.5 equiv.)	Wash twice	99.75 (R)
19	D-7 (1.0 equiv.)	DCM:PE = 13:1 (14.3 L/mol) <sup>c</sup>	- <sup>d</sup>
20	D-7 (0.5 equiv.)	DCM:PE = 13:1 (14.3 L/mol) <sup>c</sup>	- <sup>d</sup>
21	D-7 (1.5 equiv.)	DCM:n-Hex = 13:1 (14.3 L/mol) <sup>c</sup>	80.21 (R)
22	D-7 (1.5 equiv.)	Wash once	76.54 (R)
23	D-7 (1.5 equiv.)	DCM:n-pentane = 13:1 (14.3 L/mol) <sup>c</sup>	92.52 (R)
24	D-7 (1.5 equiv.)	Wash once	99.93 (R)
25	D-6 (1.5 equiv.)	DCM:PE = 13:1 (14.3 L/mol) <sup>c</sup>	- <sup>d</sup>
26	D-6 (2.0 equiv.)	DCM:PE = 13:1 (14.3 L/mol) <sup>c</sup>	- <sup>d</sup>

<sup>a</sup> The amount of *rac*-**2** was 0.30 mmol. <sup>b</sup> The amount of solvent relative to the amount of *rac*-**2** is shown within the parenthesis. <sup>c</sup> The process of heating to complete dissolution and cooling to room temperature for 2–24 h. <sup>d</sup> No crystallization. <sup>e</sup> e.e. was determined by chiral HPLC analysis.

When adding EtOH, i-PrOH, or EA in DCM (entries 8-10), there were no resolution effect. Presumably, the polar solvent might inhibit the interaction between *rac*-**2** and the resolution agents. Fortunately, when added petroleum ether (PE, boiling range is 60-90°C) in DCM (entry 11), large amounts of white precipitate appeared with low enantiomeric excess ((*R*)-**2**, e.e. = 19.54%).

After the optimization of the resolution conditions (entry 12-20), through adjustment of the ratio of DCM to PE and the initial molar ratio of *rac*-**2** to **D-7**, obvious resolution effect was

achieved (entry 16, e.e. = 87.21%). The enantiomeric excess (entry 18, e.e. = 99.75%) could be further improved by washing the precipitate twice with the corresponding solvents. The result showed that DCM was necessary to increase the solubility of the salt and provide a suitable environment for the interaction of D-7 and *rac*-2. Meanwhile, PE in the resolution solvent mixture might balance the solubility of diastereomeric salt and facilitate it to deposit.

Since PE contains mainly hexane and pentane, a mixture of DCM and n-hexane (n-Hex) was used as resolution solvent, and a fairly good resolution effect (entry 21, e.e. = 80.21%) was attained. But the optical purity could not be further raised by washing of the diastereomeric salt (entry 22). When using the DCM and n-pentane, a high resolution effect was obtained (e.e. = 92.52%) (entry 23). After simple washing, the e.e. value was remarkably increased to 99.93% (entry 24). The process of washing might just remove the residue of (*S*)-2·D-7 salt existing in the less-soluble salt of (*R*)-2·D-7. From this result, it might be inferred that the five-carbon chain of n-pentane is more suitable for the resolution of *rac*-2.

Under the optimized condition, D-6 was tried again as resolving agent, but still no precipitate appeared (entries 25, 26). Thus, it could be deduced that the methyl group of D-7 is essential for the optical resolution of *rac*-2.

### 2.3. Crystallographic analysis of (*S*)-2·L-7

To elucidate the mechanism underlying the optical resolution of *rac*-2, the crystallographic analysis of the less-soluble salt (*S*)-2·L-7 was performed. The single crystal of the (*S*)-2·L-7 salt tended to grow in ethanol after recrystallization of the diastereomeric salt isolated from DCM-PE mixture solvents. The crystallized salt consisted of (*S*)-2, L-7 and EtOH in a ratio of 1:1:2. They composed a one-dimensional  $2_1$  screw linear structure along the *a* axis supported by salt bond, hydrogen bond, CH- $\pi$  interaction, and  $\pi$ - $\pi$  interaction (Fig. 3, Fig. S1-4).

It was observed that one carboxyl group of L-7 was ionized and a salt bond between (*S*)-2 and L-7 was thus formed. The same carboxyl group bearing negative charge also formed an intermolecular hydrogen bond with another L-7 molecule (H-bond, the O...O distance was 2.566 Å). The methyl group of L-7 formed CH- $\pi$  interaction with the phenyl fragment of (*S*)-2 (The distance of C... $\pi$ -plane was 3.338 Å as shown in Fig. S2). The  $\pi$ -stacking distance is typically 3.4-3.6 Å that represents the shortest interplanar distance<sup>9</sup>. In this study, the distance between two benzyl groups of adjacent L-7 molecules was 3.441 Å, and the dihedral angle of two  $\pi$ -planes was 4.29° (Fig. S3), indicating that the  $\pi$ - $\pi$  interaction appeared between adjacent L-7 molecules. Meanwhile, the benzyl group of L-7 and the imidazole group of (*S*)-2 were located closely in space, with the distance between two  $\pi$ -planes being 3.492 Å (Fig. S4). This implied that the  $\pi$ - $\pi$  interaction stabilized the crystal structure of (*S*)-2·L-7 salt.

Each one-dimensional chain was antiparallel with their neighboring chains (Fig. 3a). For this chiral resolution, the intermolecular interactions between (*S*)-2 and the L-7 from the neighboring antiparallel one-dimensional chain were crucial. There were three CH...O interactions between antiparallel chains. The hydrogen atom of the chair carbon of (*S*)-2 formed a CH...O interaction with the ester carbonyl oxygen atom of L-7 from the same neighboring antiparallel one-dimensional chain (the CH...O distance was 2.319 Å, Fig. S5). The keto carbonyl oxygen atom of (*S*)-2 also formed a CH...O interaction with the methyl hydrogen atom of L-7 from the same neighboring

antiparallel chain (the CH...O distance was 2.478 Å) (Fig. S5). In addition, the hydrogen atom of the phenyl fragment of (*S*)-2 formed a CH...O interaction with the ester oxygen atom (the CH...O distance was 2.419 Å). All three CH...O interactions were shorter than the sum of the van der Waals radii of hydrogen and oxygen atoms 2.80 Å<sup>8c</sup>, indicating their contribution to the chiral recognition of (*S*)-2. The phenomenon that tolyl group of L-7 involved in the chiral recognition process might be the reason for the striking difference of resolution capability between D-6 and D-7. Similar situation also occurred in the optical resolution of *rac*-2-[amino(phenyl)methyl] phenol<sup>8d</sup>.

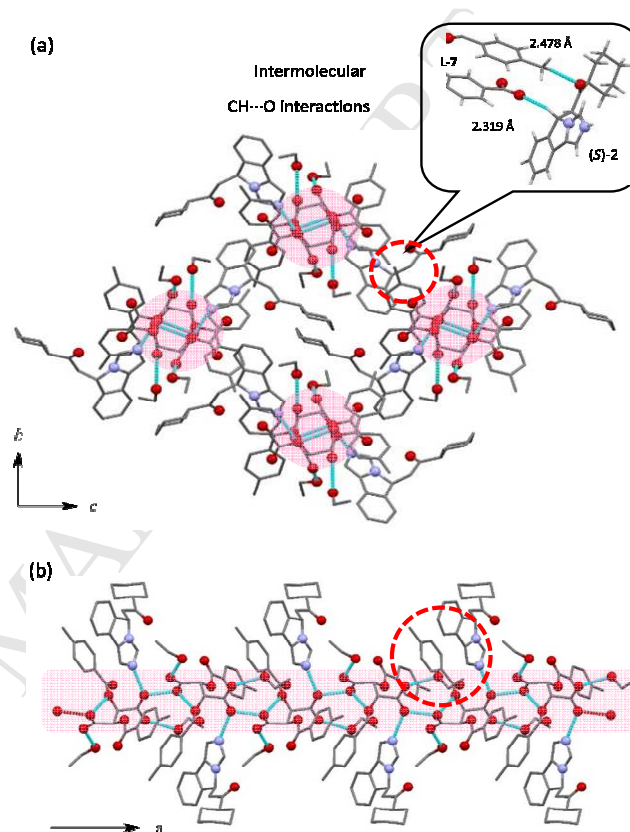


**Fig. 3.** Crystal structure of (*S*)-2·L-7·2EtOH. (a) Top view of the four linear structures viewed from a axis. Hydrogen atoms are omitted for clarity. (b) Side view of the linear structure viewed along a axis. The dotted lines and arrows show hydrogen bonds, CH...O interactions and  $\pi$ - $\pi$  interactions, respectively.

When considering the conformation of the salt unit (*S*)-2·L-7 (Fig. 4a) in the crystal, the total binding energy of (*S*)-2 and L-7 was calculated to be -387.15 kJ/mol, adopting time-dependent density functional theory (TDDFT) methodology at the B3LYP/6-31+G(d,p) basis set. Meanwhile, the calculated binding energy of (*R*)-2·L-7 salt was slightly higher (-381.10 kJ/mol), illustrating that (*S*)-2·L-7 salt was more stable than the diastereomeric counterpart.

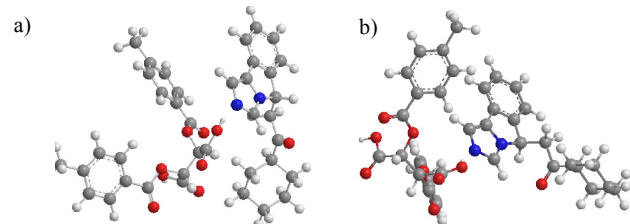


**Fig. 4.** Geometries of the diastereomeric salts. (a) (*S*)-2·L-7 and (b) (*R*)-2·L-7.

### 2.4. Effects of solvent on the optical resolution

Suitable resolution solvents could enhance the interaction between the racemic substrate and the resolution agent. In this case, the DCM-PE solvent system might provide a hydrophobic environment for the highly selective interaction between L-7 and *rac*-2. Two adjacent parallel chains might form a hydrophobic channel by the cyclohexyl group of (*S*)-2 (Fig. S6). The distance between two cyclohexyl groups of (*S*)-2 was 6.901 Å. Coincidentally, the molecular lengths of n-pentane and n-Hex were 6.793 Å and 8.047 Å, respectively (Fig. S7). It was thus inferred that the n-pentane molecule might connect cyclohexyl group through hydrophobic interaction and promote the formation and enhance the stabilization of the channel. These might also be the reason for that the PE or n-pentane could trigger the formation of the less-soluble salt in DCM, but the longer n-Hex exerted low resolving capability.

In the crystal of diastereomeric salt, EtOH only formed an H-bond with the carboxyl group of L-7. Moreover, when only EtOH was used to dissolve L-7 and (*S*)-2 for the recrystallization, no precipitate appeared. It is thus regarded that EtOH might attribute little to the chiral recognition but could promote the crystal growth of the less-soluble salt.

### 2.5. Large scale optical resolution and absolute configuration assignments of enantiopure 2

With the optimized condition in hand, we applied it to prepare the optical pure 2 in a large scale. By using two commercially available resolving agents D-7 and L-7, two enantiomers of *rac*-2 was obtained in a good efficiency in a gram scale (Table 3). Compared with DCM-PE solvent, using DCM of n-pentane solvent as resolution solvent could get better yield in a short time and with great resolution effect (e.e. > 99%, eff. up to 0.7).

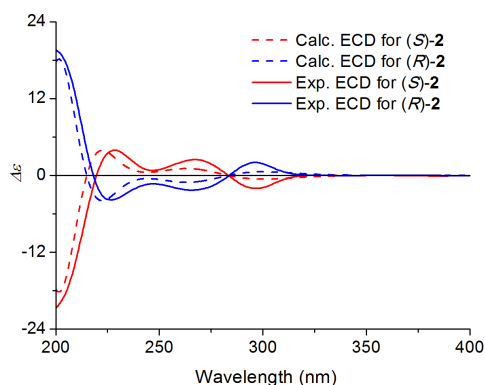


**Fig. 5.** Comparison of experimental and theoretical ECD spectra for four stereoisomers of 2.

Although the optical pure stereoisomer of 2 obtained using L-7 could be assigned as *S* configuration according to the single crystal of diastereomeric salt, it is more convincing to use another independent method to verify the stereochemical characterization. Nowadays, electronic circular dichroism (ECD)

**Table 3.** Enantioseparation of *rac*-2 with acidic resolving agents.

Entry	<i>rac</i> -2	Resolving agent	Conditions <sup>a</sup>	e.e. (%) <sup>d</sup>	Yield (%)	eff <sup>c</sup>
1	2.14 mmol	D-7 (1.5 equiv.)	DCM:PE = 13:1 (14.3 L/mol) <sup>b</sup>	98.75 ( <i>R</i> )	61	0.60
2	7.85 mmol	L-7 (1.5 equiv.)	DCM:PE = 13:1 (14.3 L/mol) <sup>b</sup>	99.61 ( <i>S</i> )	56	0.55
3	1.0 mmol	D-7 (1.5 equiv.)	DCM:n-pentane = 13:1 (14.3 L/mol) <sup>c</sup>	99.98 ( <i>R</i> )	70	0.69
4	2.85 mmol	L-7 (1.5 equiv.)	DCM:n-pentane = 13:1 (14.3 L/mol) <sup>c</sup>	99.93 ( <i>S</i> )	68	0.67

<sup>a</sup> The amount of solvent relative to the amount of *rac*-2 is shown within the parenthesis. <sup>b</sup> The process of keeping slow volatilization in room temperature for 3 to 24 h, and the precipitation was washed twice. <sup>c</sup> The process of keeping slow volatilization in room temperature for 2 to 6 h, and the precipitation was washed once or twice. <sup>d</sup> e.e. was determined by chiral HPLC analysis. <sup>e</sup> eff = e.e.% × yield%/10000.

spectra combined with TDDFT calculation has become a powerful tool to stereochemical study<sup>10</sup>. In this work, this method was also adopted to confirm the absolute configurations of enantiopure 2 (Fig. 5). Albeit slightly blue-shifted by 5 nm in the range of 280-200 nm, the calculated ECD spectra reproduced all the Cotton effects (CEs) appeared in the experimental ECD of the corresponding stereoisomer of 2.

### 2.6. Preparation and absolute configuration assignments of four stereoisomers of 1

Four diastereoisomers of 1 were prepared by the reduction of enantiopure 2, followed by the separation of the silica gel column chromatography. Stereo-selectivity was observed to occur during the reduction by NaBH<sub>4</sub>, since (*S*)-2 tended to give (*5S,2'R*)-1 and (*5S,2'S*)-1 at a ratio of 4:1. This priority might be due to the difference between steric hindrances encountered by the reduction agent from two sides of the large planar aromatic ring. Chiral HPLC analysis of *rac*-1 showed four peaks at 9.78 min, 11.93 min, 18.71 min, and 21.15 min (Fig. S9).

ECD method and quantum chemical calculation were firstly tried to establish the absolute configurations of all the stereoisomers of 1. Nevertheless, since the C2' atom is far from the aromatic chromophore and exerts little effect on the ECD spectra, two isomers with the same C5 configuration would give quite similar ECD spectra. Both experimental and theoretical ECD spectra verified the presumption (Fig. 6). When comparing the ECD spectra of optical pure 1 and 2 with the same C5 configuration, it was obvious that the C2' chirality changed the sign of the CE at 300 nm.

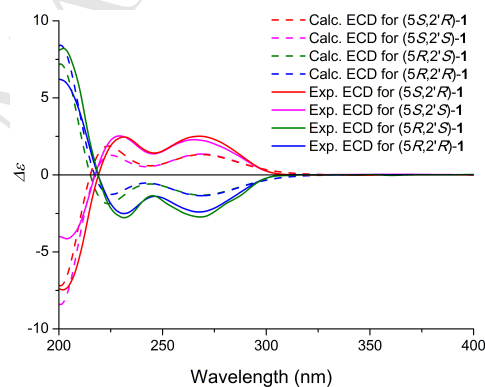


**Fig. 6.** Comparison of experimental and theoretical ECD spectra for four stereoisomers of 1.

The establishment of C2' configuration fell back on transition metal method developed for the chiral secondary alcohols<sup>11</sup>. The absolute configuration at the C2' atom could be deduced unambiguously from the induced ECD (ICD) data of the in situ-formed Rh<sub>2</sub>(CF<sub>3</sub>COO)<sub>4</sub> complexes of enantiopure 1.

The ICD of components at 11.93 min and 18.71 min displayed a positive CE at around 340 nm (Fig. 7), indicating that C2' atom on their structures could be assigned as *S* configuration. Both other peaks gave negative CEs at around 340 nm in the ICD spectra, leading to the assignments of their C2' atoms as *R* configuration. Thus, four stereoisomers were obtained, and their absolute configurations were firmly established.

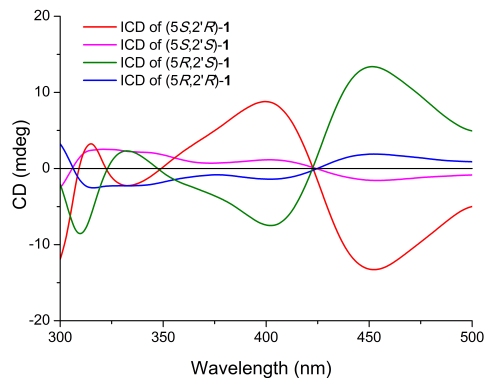


**Fig. 7.** ICD spectra induced by  $\text{Rh}_2(\text{CF}_3\text{COO})_4$  complexation with four stereoisomers of **1**.

### 2.7. Effect of stereochemistry on IDO1 inhibitory activity

The inhibitory activity assessment results of *rac-1* and its four stereoisomers against IDO1 enzymatically and in HEK293 cells are listed in Table 4. It is obvious that (5*S*,2'*R*)-**1** possessed the most potent IDO1 inhibitory activity with  $\text{IC}_{50} < 0.001 \mu\text{M}$  in both assessments. Another isomer with the same C5 configuration displayed moderate activity against IDO1, while the inhibitory activity was totally lost in the other two isomers with C5 position as *R* configuration. This result is in coincidence with Peng's report against IDO1 at the level of isolated enzyme, which showed that (5*S*,2'*R*)- and (5*S*,2'*S*)- isomers significantly contributed to the IDO1 inhibitory activity<sup>6</sup>.

**Table 4.** IDO1 inhibitory activity of *rac-1* and its stereoisomers in vitro.

Entry	$\text{IC}_{50}$ ( $\mu\text{M}$ )	
	rhIDO1	HEK293T cell
<i>rac-1</i>	0.517	0.76
(5 <i>S</i> ,2' <i>S</i> )- <b>1</b>	0.329	0.29
(5 <i>S</i> ,2' <i>R</i> )- <b>1</b>	< 0.001	< 0.001
(5 <i>R</i> ,2' <i>R</i> )- <b>1</b>	> 100	> 100
(5 <i>R</i> ,2' <i>S</i> )- <b>1</b>	> 100	> 100

**Table 5.** IDO1 inhibitory activity of *rac-1* and its stereoisomers in mouse.

Entry	Specific metabolic rate (%) <sup>a</sup>	
	0 h	1.5 h
vehicle	1.81±0.64	2.11±0.51
<i>rac-1</i>	1.42±0.22	1.24±0.08**
(5 <i>S</i> ,2' <i>S</i> )- <b>1</b>	1.66±0.27	0.79±0.15***
(5 <i>S</i> ,2' <i>R</i> )- <b>1</b>	1.45±0.10	1.01±0.07**
(5 <i>R</i> ,2' <i>R</i> )- <b>1</b>	1.33±0.35	1.36±0.20*
(5 <i>R</i> ,2' <i>S</i> )- <b>1</b>	1.61±0.26	1.53±0.27

<sup>a</sup> Specific metabolic rate (%) =  $C_{\text{Kyn}}/C_{\text{TTP}} \times 100\%$ , and values are represented as means  $\pm$  S.D. Compared with vehicle group, \*  $P < 0.05$ , \*\*  $P < 0.01$ , \*\*\*  $P < 0.001$ .

Thinking of the complexity of biological metabolism system and the original function of IDO1 enzyme, it might be reasonable and acceptable that the tremendous difference of IDO1 inhibitory activity between these stereoisomers reduced greatly in mouse (Table 5). Nevertheless, both isomers with *S* configuration at C5 position showed significant IDO1 inhibitory activity compared with vehicle group and two other isomers' groups at 1.5 h. It is thus inferred that *S* configuration at C5 position is crucial for the in vivo inhibitory activity against IDO1, while the C2' stereochemistry shows less affection.

### 3. Conclusion

In this study, we carried out the direct enantiomer separation of *rac-2* by using di-*p*-toluoyl-L-tartaric acid (L-7) in dichloromethane of petroleum ether or *n*-pentane solvent. The special solvent system provided a suitable condition for the interaction between *rac-2* and L-7, including salt bond, H-bond,  $\text{CH}\cdots\pi$  interaction,  $\text{CH}\cdots\text{O}$  interaction and  $\pi\cdots\pi$  interaction, which caused the highly selective combination and the effective resolution. Absolute configurations of all stereoisomers of **1** and **2** were assigned by single crystal X-ray diffraction, comparison of experimental and theoretical ECD spectra, and transition metal methods. The IDO inhibitory activity of each stereoisomer of **1** in vitro and in mouse plasma demonstrated that *S* configuration of C5 played great role on the IDO1 inhibitory activity, while the stereochemistry on C2' exerted little effect on the inhibitory activity of IDO1 in mouse plasma.

### 4. Experimental section

#### 4.1. Materials and methods

Reagents and solvents were purchased from Energy Chemistry, and J&K Chemical. All commercial products were used without further purification. The reactions were monitored by thin layer chromatography (TLC). The silica gel column chromatography was carried out with 300–400 mesh silica gel. Melting points were measured on a RY-2 digital melting point apparatus. Chiral HPLC analysis was performed using a Jasco LC-2000 HPLC instrument with a UV detector (MD-2010) and an auto sampler (AS-2055). Separation was implemented on Daicel Chiralpak AD-H column (4.6  $\times$  250 mm, 5 $\mu\text{m}$ ) or Daicel Chiralcel OD-H column (4.6  $\times$  250 mm, 5 $\mu\text{m}$ ). NMR spectra were recorded on Joel ECZ-400S NMR System or Bruker Avance-III 500 NMR spectrometer in  $\text{CDCl}_3$  or  $\text{DMSO}-d_6$ . ESI-MS data were collected on the Thermo Exactive Orbitrap mass spectrometer. Optical rotations were obtained using an INESA SGW-5 automatic polarimeter at D line at room temperature. ECD spectra were recorded on a Jasco J-815 spectrometer in methanol. X-ray crystallographic data were collected on an Oxford Gemini E diffractometer with graphite monochromated Cu-K $\alpha$  radiation.

#### 4.2. Synthesis of *rac-1*-cyclohexyl-2-(5*H*-imidazo[5,1-*a*]isoindol-5-yl)ethanone (*rac-2*)

The synthesis of *rac-1*-cyclohexyl-2-(5*H*-imidazo[5,1-*a*]isoindol-5-yl)ethanone (*rac-2*) followed the reported procedure with necessary modifications<sup>7</sup>. *Rac-2* was purified by silica gel column chromatography using PE and EA as elute to give *rac-2* with a yield of 51%. Yellow solid, m.p.: 80 – 81.9°C. <sup>1</sup>H NMR (400 MHz,  $\text{DMSO}-d_6$ ):  $\delta$  (ppm) 7.56 (d, 2H,  $J = 6.0$  Hz), 7.45 (d, 1H,  $J = 7.6$  Hz), 7.34 (t, 1H,  $J = 7.5$  Hz), 7.23 (t, 1H,  $J = 7.5$  Hz), 7.08 (s, 1H), 5.54 (dd, 1H,  $J = 8.4, 4.0$  Hz), 3.42 (dd, 1H,  $J = 18.8, 4.0$  Hz), 3.04 (dd, 1H,  $J = 17.6, 8.0$  Hz), 2.40 (m, 1H),

1.84 – 1.52 (m, 5H), 1.28 – 1.12 (m, 5H). ESI-HRMS: calcd for  $C_{18}H_{21}N_2O$   $[M+H]^+$  281.1648, found 281.1646.

#### 4.3. Synthesis of *rac*-5-(2-hydroxylcyclohexylethyl)-5*H*-imidazo[5,1-*a*]isoindole (*rac*-1)

The synthesis of *rac*-5-(2-hydroxylcyclohexylethyl)-5*H*-imidazo[5,1-*a*]isoindole (*rac*-1) followed the reported procedure with necessary modifications<sup>7</sup>. *Rac*-1 was purified by silica gel column chromatography using PE and EA as elute with a yield of 80%. White solid, m.p.: 158 – 159°C. <sup>1</sup>H (500 MHz, CDCl<sub>3</sub>) for a mixture of two pairs of diastereoisomers, major/minor = 4/1) δ (ppm) 7.94 (s, 1H, minor), 7.89 (s, 1H, major), 7.58 (d, *J* = 7.5 Hz, 1H), 7.48 (d, *J* = 7.5 Hz, 1H), 7.41 (t, *J* = 7.5 Hz, 1H, major), 7.38 (s, 1H, minor), 7.27 (s, 1H), 7.21 (s, 1H), 5.55 (d, *J* = 12.0 Hz, 1H, minor), 5.41 (t, *J* = 6.0 Hz, 1H, major), 3.86 – 3.80 (m, 1H, minor), 3.80 – 3.76 (m, 1H, major), 2.28(s, 1H), 2.20 – 2.18 (m, 1H), 1.80 – 1.69 (m, 5H), 1.30-1.04 (m, 6H). ESI-HRMS: calcd for  $C_{18}H_{23}N_2O$   $[M+H]^+$  283.1805, found 283.1805.

#### 4.4. Chiral resolution of *rac*-2

*Rac*-2 (2.20 g, 7.85 mmol) and resolving agent *D*-7 (4.55 g, 11.78 mmol) were dissolved in DCM (104 mL). PE (7.8 mL) was added to the mixture and stirred at room temperature for 24h. The precipitated salt was collected by filtration and washed by 20 mL DCM. The residue was then suspended in 20 mL water, and saturated Na<sub>2</sub>CO<sub>3</sub> aqueous solution was added to adjust pH value to 9-10. The solution was extracted with DCM (20 mL × 3), and dried over anhydrous Na<sub>2</sub>SO<sub>4</sub>. After removal of the solvent, (*R*)-2 (0.62 g, 2.21 mmol, 99% ee, 56% yield) was obtained as yellow oil. The yield was calculated based on a half amount of *rac*-2 initially used. The enantiomer excess was determined by chiral HPLC analysis (Daicel Chiralcel OD-H, 20°C, *n*-Hex:2-propanol = 90:10, 1.0 mL/min, *t*<sub>r</sub>(*R*) = 28.71 min, *t*<sub>r</sub>(*S*) = 20.31 min). <sup>1</sup>H NMR (400 MHz, DMSO-*d*<sub>6</sub>): δ (ppm) 7.55 (d, 2H, *J* = 7.2 Hz), 7.44 (d, 1H, *J* = 7.6 Hz), 7.34 (t, 1H, *J* = 7.6 Hz), 7.22 (t, 1H, *J* = 7.6 Hz), 7.08 (s, 1H), 5.54 (dd, 1H, *J* = 8.4, 4.0 Hz), 3.41 (dd, 1H, *J* = 18.4, 4.4 Hz), 3.03 (dd, 1H, *J* = 18.4, 8.8 Hz), 2.40 (m, 1H), 1.83 – 1.51 (m, 5H), 1.32 – 1.05 (m, 5H). <sup>13</sup>C NMR (125 MHz, DMSO-*d*<sub>6</sub>): δ (ppm) 212.11, 145.53, 137.66, 133.35, 130.05, 129.02, 124.51, 120.23, 118.59, 56.68, 56.33, 50.15, 46.72, 40.31, 28.37, 26.05, 25.66. ESI-HRMS: calcd for  $C_{18}H_{21}N_2O$   $[M+H]^+$  281.1648, found 281.1646.  $[\alpha]_D^{23} = +81.0$  (c = 0.5, CH<sub>3</sub>OH). ECD(CH<sub>3</sub>OH): Δε 296.5 (+2.03), 265.5 (–2.30), 226.5 (–3.81), 200.0 (+19.58).

By the same way, using *L*-7 as resolving agent to resolved *rac*-2 (1 g, 3.57 mmol) obtained (*S*)-2 (0.28 g, 1.00 mmol, 99% e.e., 56% yield). Yellow oil. <sup>1</sup>H NMR (400 MHz, DMSO-*d*<sub>6</sub>): δ (ppm) 7.56 (t, 2H, *J* = 4.8 Hz), 7.45 (d, 1H, *J* = 4.4 Hz), 7.34 (t, 1H, *J* = 8.0 Hz), 7.22 (t, 1H, *J* = 8.0 Hz), 7.08 (s, 1H), 5.54 (dd, 1H, *J* = 9.2, 4.8 Hz), 3.41 (dd, 1H, *J* = 18.4, 4.4 Hz), 3.04 (dd, 1H, *J* = 18.8, 8.8 Hz), 2.40 (m, 1H), 1.87 – 1.45 (m, 5H), 1.33 – 1.02 (m, 5H). <sup>13</sup>C NMR (125 MHz, DMSO-*d*<sub>6</sub>): δ (ppm) 212.90, 145.35, 137.38, 133.16, 129.86, 128.85, 126.85, 124.33, 120.05, 118.41, 56.14, 49.97, 46.53, 39.96, 28.21, 25.86, 25.48. ESI-HRMS: calcd for  $C_{18}H_{21}N_2O$   $[M+H]^+$  281.1648, found 281.1646.  $[\alpha]_D^{23} = -85.6$  (c = 0.9, CH<sub>3</sub>OH). ECD (CH<sub>3</sub>OH): Δε 296.5 (–2.03), 267.0 (+2.47), 228.5 (+3.96), 200.0 (–20.67).

#### 4.5. General procedure for the preparation of enantiopure 5-(2-hydroxylcyclohexylethyl)-5*H*-imidazo[5,1-*a*]isoindole (*1*)

Enantiopure **2** was treated in the same way as its racemate two give four enantiopure stereoisomers of **1** after silica gel column chromatography. The enantiomeric excess of each optical pure **1** was determined by an HPLC analysis (Daicel Chiralpak AD-H,

*n*-Hex/EtOH = 85:15, 20°C, 1.0 mL/min, *t*<sub>r</sub>(5*R*,2'*R*) = 9.78 min; *t*<sub>r</sub>(5*R*,2'*S*) = 11.93 min; *t*<sub>r</sub>(5*S*,2'*S*) = 18.71 min; *t*<sub>r</sub>(5*S*,2'*R*) = 21.15 min).

##### 4.5.1. (*R*)-5-((*R*)-2-hydroxylcyclohexylethyl)-5*H*-imidazo[5,1-*a*]isoindole ((5*R*,2'*R*)-*1*)

White solid, m.p.: 142 – 143°C. <sup>1</sup>H NMR (400 MHz, CDCl<sub>3</sub>): δ (ppm) 7.88 (s, 1H), 7.50 (d, *J* = 7.6 Hz, 1H), 7.36 – 7.29 (m, 2H), 7.24 – 7.19 (m, 1H), 7.15 (s, 1H), 5.49 (dd, *J* = 10.8, 2.8 Hz, 1H), 3.79-3.74 (m, 1H), 3.40 (s, 1H), 2.23 (m, 1H), 1.90 (m, 1H), 1.81 – 1.59 (m, 5H), 1.29 – 0.92 (m, 6H). <sup>13</sup>C NMR (125 MHz, CDCl<sub>3</sub>): δ (ppm) 145.50, 137.60, 132.66, 130.02, 128.56, 126.60, 124.15, 120.25, 117.89, 73.26, 59.35, 44.76, 40.96, 29.20, 28.21, 26.61, 26.38, 26.29. ESI-HRMS: calcd for  $C_{18}H_{23}N_2O$   $[M+H]^+$  283.1805, found 283.1805.  $[\alpha]_D^{23} = -20.9$  (c = 0.3, EtOH). ECD (CH<sub>3</sub>OH): Δε 267.5 (–2.41), 246.5 (–1.39), 231.5 (–2.51), 203.0 (+6.05).

##### 4.5.2. (*S*)-5-((*S*)-2-hydroxylcyclohexylethyl)-5*H*-imidazo[5,1-*a*]isoindole ((5*S*,2'*S*)-*1*)

White solid, m.p.: 141-142°C. <sup>1</sup>H NMR (400 MHz, CDCl<sub>3</sub>): δ (ppm) 7.91 (s, 1H), 7.52 (d, *J* = 7.2 Hz, 1H), 7.34 (t, *J* = 8.0 Hz, 2H), 7.23 (t, *J* = 8.0 Hz, 1H), 7.17 (s, 1H), 5.49 (dd, *J* = 10.4, 2.8 Hz, 1H), 3.78 (m, 1H), 2.95 (s, 1H), 2.27-2.19 (m, 1H), 1.89-1.86 (m, 1H), 1.83 – 1.59 (m, 5H), 1.30 – 0.93 (m, 6H). <sup>13</sup>C NMR (125 MHz, CDCl<sub>3</sub>): δ (ppm) 146.05, 137.91, 133.37, 129.80, 128.50, 126.79, 123.35, 120.26, 117.78, 71.19, 58.52, 44.77, 39.72, 29.04, 28.51, 26.57, 26.25, 18.66. ESI-HRMS: calcd for  $C_{18}H_{23}N_2O$   $[M+H]^+$  283.1805, found 283.1805.  $[\alpha]_D^{23} = +21.1$  (c = 0.6, EtOH). ECD (CH<sub>3</sub>OH): Δε 265.0 (+2.28), 245.5 (+1.37), 229.5 (+2.52), 204.0 (–4.15).

##### 4.5.3. (*S*)-5-((*R*)-2-hydroxylcyclohexylethyl)-5*H*-imidazo[5,1-*a*]isoindole ((5*R*,2'*S*)-*1*)

White solid, m.p.: 139 – 140°C. <sup>1</sup>H NMR (400 MHz, CDCl<sub>3</sub>): δ (ppm) 7.81 (s, 1H), 7.49 (d, *J* = 7.2 Hz, 1H), 7.42 (d, *J* = 7.6 Hz, 1H), 7.32 (t, *J* = 7.6 Hz, 1H), 7.20 (t, *J* = 7.6 Hz, 1H), 7.11 (s, 1H), 5.35 (t, *J* = 6.4 Hz, 1H), 3.79 – 3.70 (m, 1H), 3.15 (s, 1H), 2.13 (m, 1H), 2.01 (m, 1H), 1.74 (m, 5H), 1.29 – 0.88 (m, 6H). <sup>13</sup>C NMR (125 MHz, CDCl<sub>3</sub>): δ (ppm) 145.50, 137.60, 132.66, 130.02, 128.56, 126.60, 124.15, 120.25, 117.89, 73.26, 59.35, 44.76, 40.96, 29.20, 28.21, 26.61, 26.38, 26.29. ESI-HRMS: calcd for  $C_{18}H_{23}N_2O$   $[M+H]^+$  283.1805 found 283.1805.  $[\alpha]_D^{23} = -38.2$  (c = 0.6, EtOH). ECD (CH<sub>3</sub>OH): Δε 268.0 (–2.73), 245.0 (–1.35), 231.5 (–2.78), 202.0 (+8.21).

##### 4.5.4. (*R*)-5-((*S*)-2-hydroxylcyclohexylethyl)-5*H*-imidazo[5,1-*a*]isoindole ((5*S*,2'*R*)-*1*)

White solid, m.p.: 139 – 141°C. <sup>1</sup>H NMR (400 MHz, CDCl<sub>3</sub>): δ (ppm) 7.95 (s, 1H), 7.54 (d, *J* = 7.6 Hz, 1H), 7.43 (d, *J* = 7.6 Hz, 1H), 7.36 (t, *J* = 7.2 Hz, 1H), 7.27-7.23 (m, 1H), 7.17 (s, 1H), 5.38 (t, *J* = 6.0 Hz, 1H), 3.77 – 3.69 (m, 1H), 2.21 – 1.94 (m, 2H), 1.85 – 1.59 (m, 5H), 1.46 – 0.82 (m, 6H). <sup>13</sup>C NMR (125 MHz, CDCl<sub>3</sub>): δ (ppm) 145.25, 137.64, 132.68, 129.92, 128.76, 126.84, 124.12, 117.47, 120.45, 77.49, 73.60, 59.59, 44.63, 40.62, 29.11, 28.01, 26.55, 26.20, 18.65. ESI-HRMS: calcd for  $C_{18}H_{23}N_2O$   $[M+H]^+$  283.1805, found 283.1805.  $[\alpha]_D^{23} = +38.8$  (c = 0.7, EtOH). ECD (CH<sub>3</sub>OH): Δε 267.5 (+2.51), 246.0 (+1.42), 231.5 (+2.46), 203.0 (–7.43).

#### 4.6. Single crystal X-ray analysis

X-ray crystallographic data were collected on the Oxford Gemini E diffractometer with graphite monochromated Cu-Kα radiation. The structure was solved by a direct method using Shelx97 and refined by SHELXL-2014/7 program. Crystal data for (*S*)-2-*L*-7-2EtOH: C<sub>42</sub>H<sub>50</sub>N<sub>2</sub>O<sub>11</sub>, M = 758.84, orthorhombic, *a*

$a = 13.3264(7) \text{ \AA}$ ,  $b = 15.6600(11) \text{ \AA}$ ,  $c = 19.3842(10) \text{ \AA}$ ,  $U = 4045.3(4) \text{ \AA}^3$ ,  $T = 106.5 \text{ K}$ , space group  $P2_12_12_1$ ,  $\mu(\text{Cu K}\alpha) = 0.741$ ,  $Z = 4$ , 13929 reflections measured, 7637 unique ( $R_{\text{int}} = 0.0221$ ) which were used in all calculations. The final  $wR(F2)$  was 0.1004 (all data). Crystallographic data for the structures in this paper with deposition numbers CCDC 1570864 can be obtained free of charge from the Cambridge Crystallographic Data Centre via <https://www.ccdc.cam.ac.uk/structures/>.

#### 4.7. Quantum-chemical calculation

Absolute configurations at C5 atom on enantiopure **1** and **2** were assigned by comparison of experimental ECD spectra with their theoretical ECD spectra obtained by quantum-chemical calculations using Gaussian 09. Conformational analysis and ECD calculations were carried out according to the previously reported protocols<sup>12</sup>. For each main stable conformer (Boltzmann distribution > 1%), sixty lowest electronic transitions were obtained using combinations of hybrid functionals and basis sets including B3LYP/6-31+G(d,p) and Cam-B3LYP/6-31+G(d,p) approaches. Solvent effects were taken into consideration by using polarizable continuum model (PCM) for methanol using the dielectric constants of 32.613. The overall ECD spectra were then gained at the bandwidth  $\sigma = 0.35 \text{ eV}$  according to the Boltzmann average of each conformer.

#### 4.8. IDO1 inhibitory activity assessment

##### 4.8.1. Enzyme-based IDO1 inhibitory activity assay

The inhibitory activity of the compounds against IDO-1 was determined as previously reported<sup>13</sup>. A standard reaction mixture (100  $\mu\text{L}$ ) containing 0.05  $\mu\text{M}$  rhIDO-1, 200  $\mu\text{g}/\text{mL}$  catalase, 20  $\mu\text{M}$  methylene blue, 100 mM potassium phosphate buffer (pH 6.5), and 40 mM ascorbic acid (neutralized with NaOH) was added to the solution containing the substrate L-Trp and the test sample at a determined concentration. The reaction was performed at 37 °C for 45 min and stopped by adding 20  $\mu\text{L}$  of 30% (w/v) trichloroacetic acid. After heating at 65 °C for 15 min, 100  $\mu\text{L}$  of 2% (w/v) p-dimethylaminobenzaldehyde (DMAB) in acetic acid was added to each well. The yellow pigment derived from Kyn was measured at 492 nm using a Synergy-H1 microplate reader (BioTek). IC<sub>50</sub> was analyzed using the GraphPad Prism 6.

##### 4.8.2. HEK293T cell-based IDO1 inhibitory assay

The assay was performed according to a reported method<sup>13</sup>. HEK293 cells were seeded in a 96-well culture plate at a density of  $2 \times 10^4$  cells/well and cultured overnight. The HEK293 cells were then transfected with pcDNA3.1-hIDO-1 using Lipofectamin 3000 according to the manufacturer's instructions. At 16 h after transfection, a serial dilution of the tested compounds in 200  $\mu\text{L}$  culture medium was added to the cells. After an additional 24 h incubation, 100  $\mu\text{L}$  of the supernatant per well was transferred to a new 96-well plate and mixed with 20  $\mu\text{L}$  of 30% trichloroacetic acid in each well. The plate was incubated at 65 °C for 15 min to hydrolyze N-formyl Kyn produced by the catalytic reaction of IDO-1. Then, 100  $\mu\text{L}$  of 2% (w/v) DMAB in acetic acid was added to each well. The yellow color derived from Kyn was measured at 492 nm using a Synergy-H1 microplate reader (BioTek).

##### 4.8.3. IDO1 inhibitory activity assay in mouse plasma

Male C57 mice (14-16g) were bought from Beijing Vital River Laboratory Animal Technology Co. Ltd. The assay was performed as literature<sup>14</sup>. The establishment of standard curve was carried out by different concentration of working liquid of Trp and Kyn. The solution of Trp and Kyn were prepared as 20

$\mu\text{M}$  using 50% acetonitrile. The pure water with different concentration of Trp and Kyn solution (10  $\mu\text{L}$ ) and the internal standard (Inderal, 0.2  $\mu\text{g}/\text{mL}$ , 170  $\mu\text{L}$ ) were mixed, followed by the centrifugation (14000 rpm  $\times$  5 min) twice. The supernate (3  $\mu\text{L}$ ) was analyzed by LC/MS/MS, the condition of which was as follows: Zobax C18 (2.1 mm  $\times$  100 mm, 3.5  $\mu\text{m}$ ) column, 37 °C, acetonitrile/water (0.1% formic acid), 0.2 mL/min,  $m/z$  204.9  $\rightarrow$  188 (Trp),  $m/z$  208.8  $\rightarrow$  192.1 (Kyn),  $m/z$  260  $\rightarrow$  183 (Inderal as internal standard).

Thirty mice were divided randomly into six groups. Five groups were fed respectively by 9 mg/mL 0.5% CMC suspension of five tested samples, in which tween was used for the assisted dissolution. Orbital blood collection was carried out immediately and after 1.5 h. The serum samples (10  $\mu\text{L}$ ), 20  $\mu\text{L}$  acetonitrile and the internal standard (Inderal, 0.2  $\mu\text{g}/\text{mL}$ , 170  $\mu\text{L}$ ) were mixed, followed by the centrifugation (14000 rpm  $\times$  5 min) twice. The supernate (3  $\mu\text{L}$ ) was analyzed by LC/MS/MS.

#### Supplementary Materia

Single crystal X-ray diffraction, chiral HPLC analysis, NMR, and ESI-HRMS spectra for compounds **1-2** are included. This material is available free of charge via the Internet at <https://>.

#### Acknowledgments

This study was financially supported by the CAMS Innovation Fund for Medical Sciences (CIFMS, No. 2016-I2M-3-009).

#### References and notes

- (a) Mahoney KM, Rennert PD, Freeman GJ. *Nat Rev Drug Discov.* 2015; 14: 561–584; (b) Topalian SL, Taube JM, Anders RA, Pardoll DM. *Nat Rev Cancer.* 2016; 16: 275–287.
- Sharma P, Allison JP. *Science.* 2015; 348: 56–61.
- Sugimoto H, Oda S, Otsuki T, Hino T, Yoshida T, Shiro Y. *P Natl Acad Sci USA.* 2006; 103: 2611–2616.
- Moyer BJ, Rojas IY, Murray IA, Lee S, Hazlett HF, Perdew GH, Tomlinson CR. *Toxicol Appl Pharm.* 2017; 323: 74–80.
- (a) Toogood PL. *Bioorg Med Chem Lett.* 2018; 28: 319–329; (b) Chen Y, Xia R, Huang Y, Zhao W, Li J, Zhang X, Wang P, Venkataramanan R, Fan J, Xie W, Ma X, Lu B, Li S. *Nat Commun.* 2016; 7: 13443; (c) Zhang G, Xing J, Wang Y, Wang L, Ye Y, Lu D, Zhao J, Luo X, Zheng M, Yan S. *Front Pharmacol.* 2018; 9: 277.
- Peng YH, Ueng SH, Tseng CT, Hung MS, Song JS, Wu JS, Liao FY, Fan YS, Wu MH, Hsiao WC, Hsueh CC, Lin SY, Cheng CY, Tu CH, Lee LC, Cheng MF, Shia KS, Shih C, Wu SY. *J Med Chem.* 2016; 59: 282–293.
- Mautino M, Kumar S, Jaipuri F, Waldo J, Kesharwani T, Zhang X. U.S. Patent 9 260 434, 2016.
- (a) Fumagalli L, Bolchi C, Bavo F, Pallavicini M. *Tetrahedron Lett.* 2016; 57: 2009–2011; (b) Zhu Q, Wang J, Bian X, Zhang L, Wei P, Xu Y. *Org Process Res Dev.* 2015; 19: 1263–1267; (c) Kodama K, Hayashi N, Fujita M, Hirose T. *RSC Adv.* 2014; 4: 25609–25615; (d) Kodama K, Hayashi N, Yoshida Y, Hirose T. *Tetrahedron.* 2016; 72: 1387–1394.
- Curtis MD, Cao J, Kampf JW. *J Am Chem Soc.* 2004; 126: 4318–4328.
- (a) Pescitelli G, Bruhn T. *Chirality.* 2016; 28: 466–474; (b) Ma K, Li L, Bao L, He L, Sun C, Zhou B, Si SY, Liu HW. *Tetrahedron.* 2015; 71: 1808–1814.
- Frelek J, Pakulski, Z, Zamojski, A. *J. Carbohydr. Chem.* 1993; 12: 625–639.
- (a) Li B, Zhang J, Yang BB, Li L, Yang XX. *RSC Adv.* 2017; 7: 45714–45720; (b) Li L, Li C, Si YK. *Chin Chem Lett.* 2013; 24: 500–502; (c) Li L, Yang BB, Si YK. *Chin Chem Lett.* 2014; 25: 1586–1590.
- Yu CJ, Zheng MF, Kuang CX, Huang WD, Yang Q. *J. Alzheimers. Dis.* 2010; 22: 257–266.
- Koblish HK, Hansbury MJ, Bowman KJ, Yang G, Neilan CL, Haley PJ, Burn TC, Waeltz P, Sparks RB, Yue EW, Combs AP, Scherle PA, Vaddi K, Fridman JS. *Mol Cancer Ther.* 2010; 9: 489–498.